# Integrated Capture and Solar-driven Utilization of $CO_2$ from Flue Gas and Air

Sayan Kar,[‡] Motiar Rahaman,[‡] Virgil Andrei, Subhajit Bhattacharjee, Souvik Roy, and Erwin Reisner*

*Yusuf Hamied Department of Chemistry, University of Cambridge, Lensfield Road, Cambridge CB2 1EW, United Kingdom*

[‡]These authors contributed equally.

*Corresponding author
Prof. Erwin Reisner
Postal address: *Yusuf Hamied Department of Chemistry, University of Cambridge, Lensfield Road, Cambridge CB2 1EW, UK*
E-mail: reisner@ch.cam.ac.uk
Tel: +44-1223336323
Website: http://www-reisner.ch.cam.ac.uk

**SUMMARY**
Integration of carbon capture with utilization technologies can lead the way to a net-zero carbon economy. Nevertheless, direct chemical conversion of captured $CO_2$ products remains challenging due to their thermodynamic stability. Here, we demonstrate $CO_2$ capture from flue gas/air and its direct conversion into syngas under solar irradiation without any externally applied voltage. The system captures $CO_2$ with an amine/hydroxide solution and photoelectrochemically converts it into syngas (CO:$H_2$ 1:2 (concentrated $CO_2$), 1:4 (simulated flue gas), and 1:30 (air)) using a perovskite-based photocathode with an immobilized molecular Co-phthalocyanine catalyst. At the anode, plastic-derived ethylene glycol is oxidized into glycolic acid over a $Cu_{26}Pd_{74}$ alloy catalyst. The overall process uses flue gas/air as carbon source and discarded plastic waste as electron donor, opening avenues for integrated carbon-neutral/negative solar fuel and waste upcycling technologies.

## INTRODUCTION

Mitigation of anthropogenic $CO_2$ accumulation is essential to tackle the current climate change and loss of biodiversity.[1] Large scale global efforts are ongoing to develop $CO_2$ conversion technologies for green fuel production.[2] Solar-driven $CO_2$ conversion is a promising approach to produce clean fuels and chemicals as it directly utilizes sunlight as the sole energy input.[3-5] However, current $CO_2$ utilization processes depend on pure and pressurized $CO_2$ as reactant, whose production from post-combustion emission streams and air is energy intensive (~2 GJ $ton_{CO2}^{-1}$ or 100 kJ $mol_{CO2}^{-1}$).[6,7] Majority of this energy demand (~80%) is from desorption and compression steps following $CO_2$ capture, involving heating large volumes of alkanolamine solutions and subsequent pressurization of the released gas (**Figure 1a**).[8,9] Direct solar-driven utilization of captured $CO_2$ species is therefore a more attractive way to reach net-zero carbon cycle, but barely explored due to their thermodynamic stability.[10,11,12,13] Thermo-catalytic hydrogenation of captured $CO_2$ has recently been reported at elevated temperatures (100–150 $^oC$).[14-16] Electrochemical reduction of alkanolamine captured $CO_2$ can also be achieved over metallic electrodes (Ag, Cu, etc.) at ambient temperatures.[17-20] Recent studies have shown small-scale localized *in situ* $CO_2$ gas adsorption followed by photocatalytic conversion in homogeneous and colloidal solutions.[21-23] Nevertheless, sunlight-driven direct capture and utilization processes with industrially relevant amine/hydroxide capturing agents is lacking, presumably due to the overwhelming energy barrier to activate the trapped $CO_2$-adducts (**Figure S1**).[24]

Here we report an integrated $CO_2$ capture and solar-driven photoelectrochemical (PEC) utilization process to produce syngas (mixture of CO and $H_2$), a precursor for industrial liquid fuels and chemicals syntheses,[25] from concentrated $CO_2$ stream, simulated post-combustion flue gas, and atmospheric air. The process operates by combining $CO_2$-to-fuel reduction with selective oxidation of waste plastic-derived ethylene glycol (EG) to glycolic acid (GA), which has applications in pharmaceutical, food and textile industries (**Figure 1b**). The system captures $CO_2$ in an aqueous amine or glycolic hydroxide solution and the subsequent PEC conversion occurs in a two-compartment, two-electrode reactor equipped with a triple cation perovskite-based photocathode. Captured $CO_2$ reduction is enabled by an immobilized molecular Co-phthalocyanine catalyst at the photocathode. A bimetallic $Cu_{26}Pd_{74}$ alloy anode completes the circuit by catalyzing EG oxidation. Replacing anodic water oxidation ($\Delta G^0(H_2O/O_2)$ = +237 kJ $mol^{-1}$) by EG oxidation ($\Delta G^0$(EG/GA) ~ +20 kJ $mol^{-1}$)[26] makes the demanding captured $CO_2$ reduction feasible with only sunlight, enabling the system to function even with a single visible-light absorber without any external applied voltage, with simultaneous waste valorization.

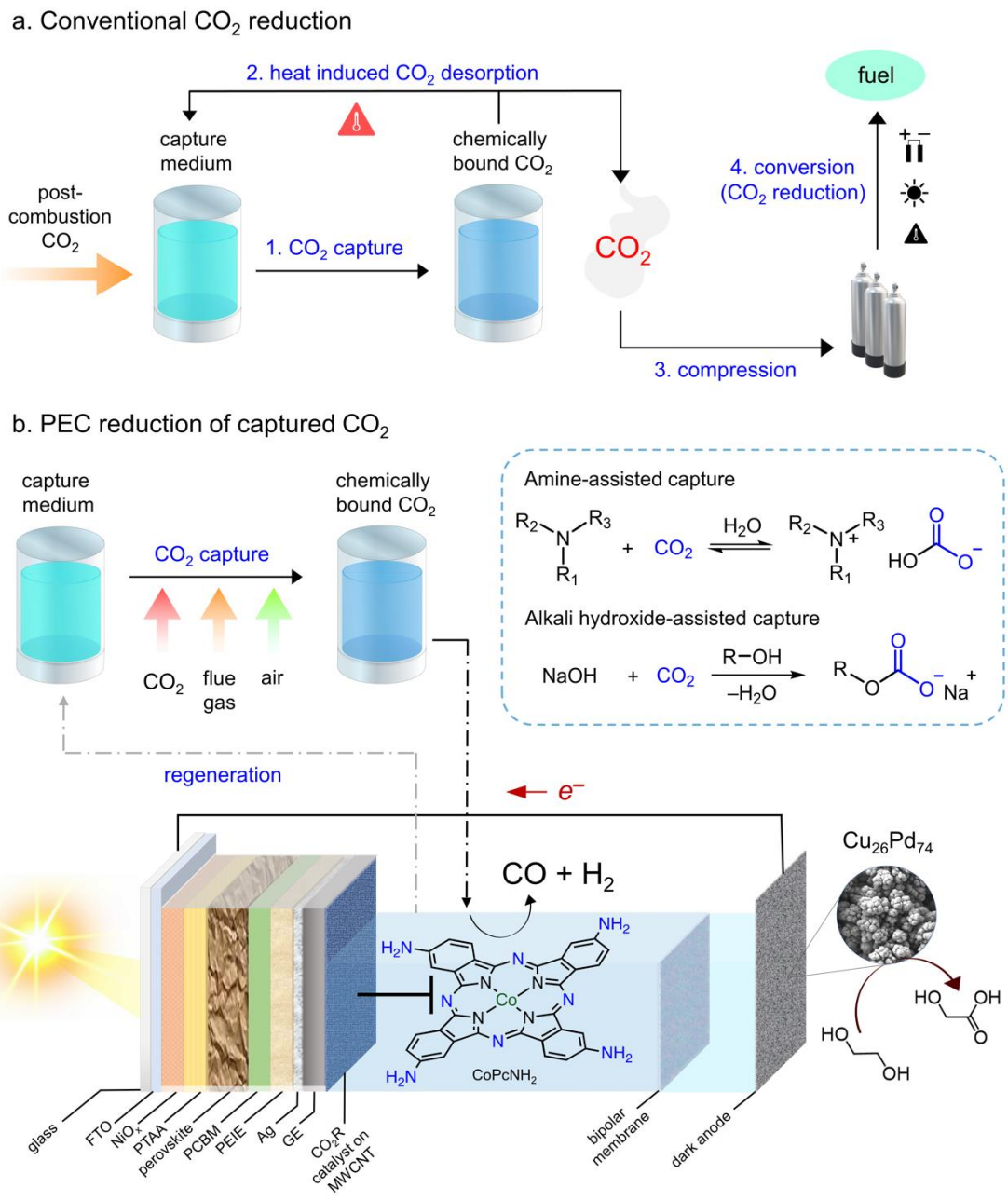


**Figure 1. Schematic representation of integrated $CO_2$ capture and conversion. a**, Conventional multi-stage CCU pathway, where $CO_2$ is first captured from post-combustion gases (step 1), followed by heat treatment to desorb $CO_2$ (step 2). The released $CO_2$ is then compressed and subsequently used for conversion (steps 3 and 4). **b**, Integrated one-step photoelectrochemical (PEC) approach reported in this study, where the post-capture solution is directly used for conversion using solar energy, to generate syngas as energy vector while at the same time upcycling plastic waste derived ethylene glycol to the commodity chemical glycolic acid. The abbreviations for the individual photocathode layers are in the Method section.

## RESULTS AND DISCUSSION

### $CO_2$ Capture

A concentrated $CO_2$ stream (99.995%) was first used to develop and optimize the PEC system. Different amines, including industrially-relevant monoethanolamine (MEA), diethanolamine (DEA), triethanolamine (TEA) and diazabicyclo[2,2,2]octane (DABCO) were employed for $CO_2$ capture in aqueous medium at ambient temperature. The capture was done by purging concentrated $CO_2$ through 1 M amine solution for 2 h (flowrate: 30 mL $min^{-1}$). The solution was further purged with $N_2$ (15 min) to remove any physically dissolved $CO_2$ **(Figure S2)**. $^{13}C$ nuclear magnetic resonance ($^{13}C$-NMR) spectra of the post-capture solutions revealed that under these conditions, MEA and DEA captured 0.75±0.07 and 0.77±0.10 mol $CO_2$ per mol amine, respectively, as bicarbonate and carbamate species.[27] In contrast, the tertiary amines TEA and DABCO captured $CO_2$ only as bicarbonate salts (0.60±0.05 and 0.85±0.08 mol $CO_2$ per mol amine, respectively, after 2 h; **Scheme 1, eq 1-2; Figure S3)**. Other than amines, aqueous and organic solutions of NaOH were also used for efficient $CO_2$ capture (**Scheme 1, eq 3**).[28] When concentrated $CO_2$ was purged through an aqueous 1 M NaOH solution (2 h), $NaHCO_3$ was formed quantitatively.[29,30] Similarly, 1 M NaOH solution in organic EG captured 0.96±0.02 mol $CO_2$ per mol NaOH as sodium glycol carbonate upon $CO_2$ purging (**Scheme 1, eq 4; Figure S4**). The $CO_2$ captured species thus obtained were subsequently for conversion.

**Scheme 1.** Aqueous and organic systems used for $CO_2$ capture

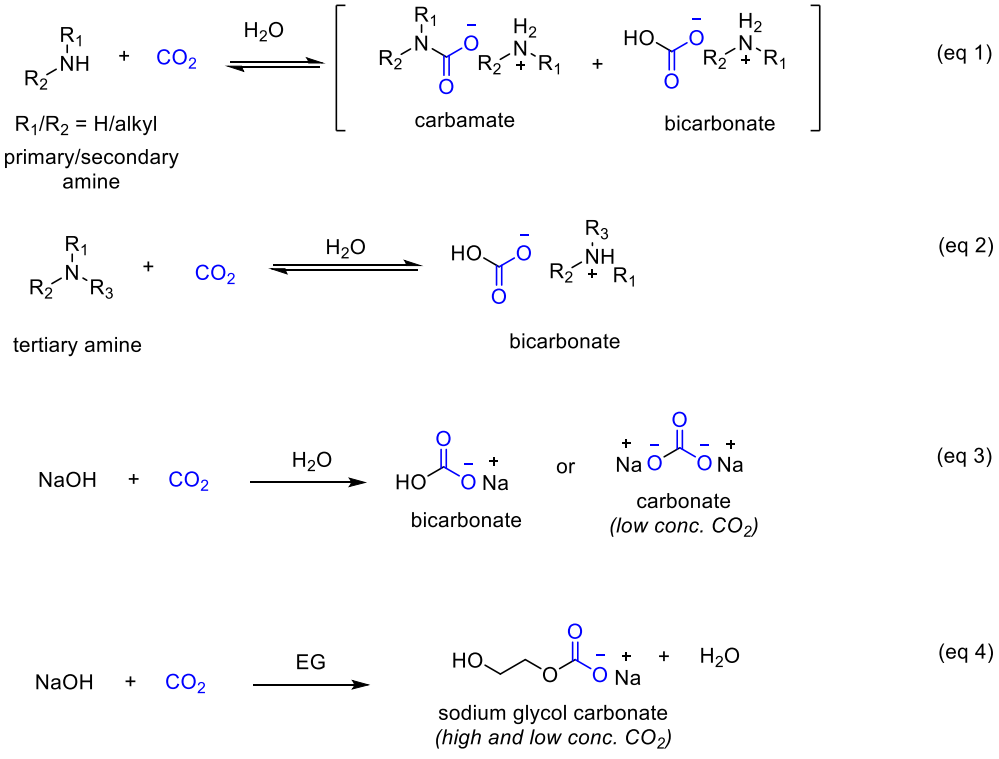


### Electrochemical characterization of captured $CO_2$ reduction

For captured $CO_2$ reduction, a tetramine substituted cobalt(II) phthalocyanine molecular catalyst ($CoPcNH_2$, **Figure 1b**) was used for its ability to form syngas at low overpotentials.[31] It was synthesized from a tetranitro precursor by sodium sulfide mediated reduction (see Methods;

**Figure S5**).[31] Electrodes were prepared by first immobilizing $CoPcNH_2$ on multi-walled carbon nanotubes (MWCNT) through π-π stacking, followed by drop-casting the composite on a graphite foil substrate ($CoPcNH_2$@MWCNT; **Figures S6-S9**).[32] Electrochemical reduction of aqueous captured $CO_2$ solutions were then explored in a two-compartment, three-electrode configuration with the fabricated $CoPcNH_2$@MWCNT electrode, a Ag/AgCl (sat. NaCl) electrode, and a Pt mesh as the working, reference, and counter (water oxidation) electrode, respectively. The catholyte was $CO_2$ captured solutions with 0.1 M $K_2SO_4$ (supporting electrolyte; pH 7.8–8.3), the anolyte was 0.1 M $K_2SO_4$ (pH 7.6), and the compartments were separated by a bipolar membrane. Cyclic voltammetry (CV) scans in a TEA (1 M) captured $CO_2$ medium in this setup showed an onset potential of –0.4 V vs. the reversible hydrogen electrode (RHE; **Figures 2a, S10)**. Subsequent controlled potential electrolysis (CPE) at different potentials (1 h) produced only CO and $H_2$ as products (**Figure 2b**). The formed bicarbonate C–O bond during $CO_2$ capture is thus cleaved during reduction, regenerating the amine. An optimum CO faradaic efficiency ($FE_{CO}$) of 46.2±2.0 % was obtained at –0.7 V vs. RHE **(Figure 2b)**. CPE with the primary and secondary amine (MEA and DEA) captured $CO_2$ solutions at this potential resulted in lower $FE_{CO}$ of 10.2±1.7 and 16.5±1.5%, respectively (**Figure 2c**). Control experiments without an amine did not capture $CO_2$ and consequently, produced no CO during CPE, confirming the role of amine in the CCU process (**Figure 2c**).

Electrochemical reduction of aqueous NaOH captured $CO_2$ species ($NaHCO_3$, $Na_2CO_3$) at –0.7 V vs. RHE showed poor $FE_{CO}$ (<3%, **Figure 2d**). Reduction of the captured $CO_2$ in glycolic NaOH solution (**Scheme 1, eq 4**) was hence explored, after adding tetrabutylammonium tetrafluoroborate ($TBABF_4$, 0.15 M) as supporting electrolyte and 20% v/v MeCN as co-solvent to ensure a homogeneous solution. The $CoPcNH_2$@MWCNT catalyst, a $Cu_xPd_y$ alloy, and a $Ag/AgNO_3$ (0.1 M *n*-$Bu_4NPF_6$ in MeCN) electrode was used as working, counter (EG oxidation), and reference electrode, respectively, and the applied potentials were converted to the $Fc/Fc^+$ scale. CV scans in this medium showed an onset potential of –1.7 V vs. $Fc/Fc^+$. Subsequent CPE studies (for 10 h) revealed an optimum CO production at –1.85 V vs. $Fc/Fc^+$ with 19.0±1.4% $FE_{CO}$ (**Figures 2e, S11)**. Isotopic labelling experiments with captured $^{13}CO_2$ in both the aqueous ($TEA/H_2O$) and non-aqueous (NaOH/EG) medium showed only $^{13}C$ labelled CO as reduction product during FTIR analysis of the headspace gas, confirming that CO was derived from captured $CO_2$ (**Figure 2f**).

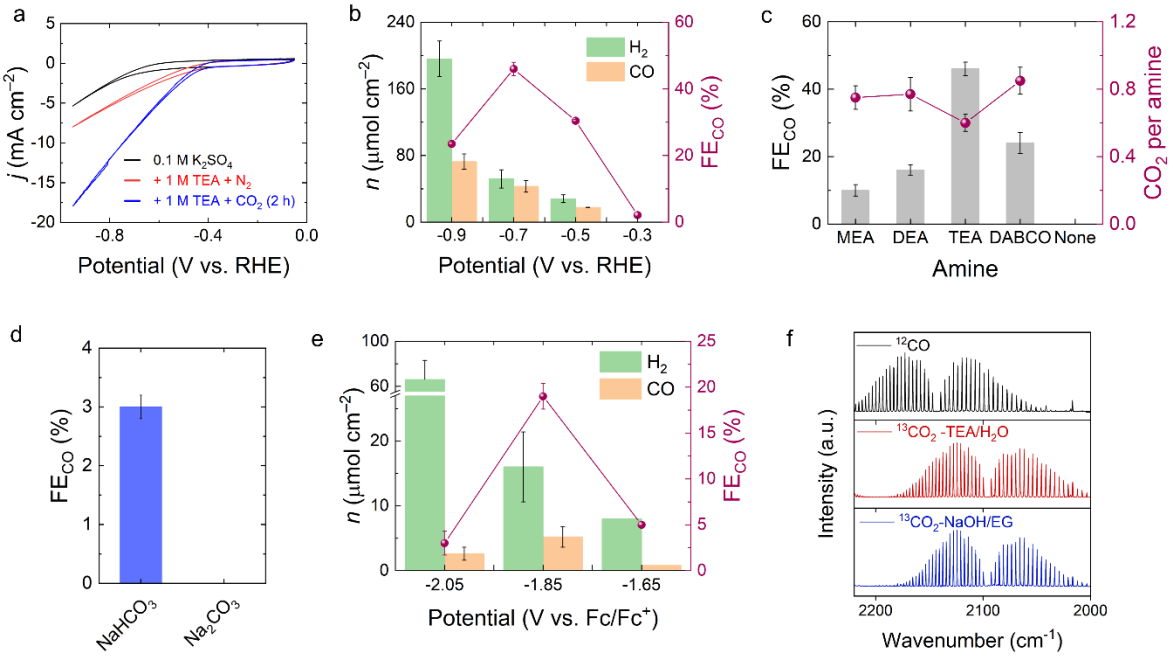


**Figure 2. Electrochemical reduction of captured $CO_2$ with $CoPcNH_2$@MWCNT electrode. a**, Cyclic voltammetry (CV) scan of triethanolamine (TEA) captured $CO_2$ and fresh TEA solution in $N_2$ (scan rate 50 mV $s^{-1}$) with $CoPcNH_2$@MWCNT cathode in a two–compartment three–electrode configuration. **b**, Product amount (normalized to geometric surface area of the electrode) and CO faradic efficiency ($FE_{CO}$) for TEA captured $CO_2$ reduction at different potentials with $CoPcNH_2$@MWCNT electrode. **c**, Captured $CO_2$ amount ($CO_2$ flowrate 30 mL $min^{-1}$; capture duration, 2 h), and observed $FE_{CO}$ for different amines after controlled potential electrolysis (CPE) at –0.7 V vs. the reversible hydrogen electrode (RHE) for 1 h (conditions for a-c: Catholyte, capture solution with 0.1 M added $K_2SO_4$; anolyte, 0.1 M $K_2SO_4$; cathode, $CoPcNH_2$@MWCNT; anode, Pt mesh; bipolar membrane). **d**, $FE_{CO}$ for reduction of NaOH captured $CO_2$ products in aqueous medium at –0.7 V vs. RHE for 1 h. **e**, $FE_{CO}$ obtained after CPE of $CO_2$ captured by glycolic NaOH solution at different potentials (conditions: catholyte, capture solution with added 20% v/v MeCN and 0.15 M tetrabutylammonium tetrafluoroborate ($TBABF_4$); anolyte, 0.6 M NaOH, 0.15 M $TBABF_4$ in 20% v/v MeCN in ethylene glycol (EG); cathode, $CoPcNH_2$@MWCNT; anode, $Cu_{26}Pd_{74}$ alloy; bipolar membrane). **f**, Fourier transform infra-red (FTIR) spectra of the headspace (CO region) after isotope labelling experiments with both TEA/$H_2O$ and NaOH/EG system using captured $^{13}CO_2$ as reactant where the $^{12}CO$ signal was obtained from an experiment with captured $^{12}CO_2$. All experiments were carried out at room temperature.

## Solar-driven conversion of captured $CO_2$

The solar-driven conversion of captured $CO_2$ (in TEA/$H_2O$ and NaOH/EG solutions, using concentrated stream) was then explored in a two-compartment cell. A photocathode was prepared for this purpose by interfacing the $CoPcNH_2$@MWCNT catalyst with a triple cation lead halide perovskite (PVK) photoabsorber using a conducting graphite epoxy paste (PVK|$CoPcNH_2$@MWCNT, Methods).[33,34] The PVK has optimal bandgap (1.6–1.7 eV) to absorb broad-range of the solar spectrum (360–750 nm), and provides high open-circuit photovoltage (~1.1 V) to efficiently drive both half-reactions.[35-37] A bimetallic $Cu_{26}Pd_{74}$ alloy electrodeposited on Ni foam substrate (Ni foam|$Cu_{26}Pd_{74}$, see Methods) was used as anode (**Figure S12-S13)**, which facilitates alcohol oxidation under alkaline conditions.[5] Operating

conditions of the two-electrode PEC setup without external bias was determined from the overlap of individual CV curves of PVK|$CoPcNH_2$@MWCNT photocathode (taken under 1 sun, AM 1.5G irradiation) and Ni foam|$Cu_{26}Pd_{74}$ anode (taken under 'dark' conditions) in three-electrode configuration **(Figures S14-S17)**. The overlap potentials ($V_{overlap}$) were 0.52 V vs. RHE and –0.85 V vs. $Fc/Fc^+$ in the TEA/$H_2O$ and NaOH/EG medium, with overlap current densities of 5.8 mA $cm^{-2}$ and 0.27 mA $cm^{-2}$, respectively (**Figures S15** and **S17**). Accounting for the open circuit voltage ($V_{OC}$) of the PVK devices (~1.05±0.03 V, **Figure S18**), the potential experienced by $CoPcNH_2$@MWCNT catalyst in the two-electrode setup without any external voltage is around –0.53 V vs. RHE and –1.9 V vs. $Fc/Fc^+$ in the TEA/$H_2O$ and NaOH/EG medium, respectively (calculated as $V_{overlap}$–$V_{OC}$). Electrochemical analyses at these potentials confirmed activity of the $CoPcNH_2$@MWCNT catalyst towards captured $CO_2$ conversion (**Figures 2b, 2e**).

For two-electrode PEC captured $CO_2$ conversion coupled to EG oxidation, the catholytes were captured $CO_2$ solution with additives (similar to **Figure 2**) and the anolytes were 0.5 M EG in 0.5 M aqueous KOH (TEA/$H_2O$) or 0.6 M NaOH, 0.15 M $TBABF_4$ in 80/20 EG/MeCN solution (NaOH/EG). The two compartments were separated by a bipolar membrane to maintain the pH difference which introduced a chemical bias (~0.35 V) to the system. CV scans under solar-irradiation showed an onset voltage at –0.4 V for the TEA/$H_2O$ system with j ~4.9 mA $cm^{-2}$ at zero applied voltage (**Figure 3a**). A stable photocurrent density of 1.1±0.3 mA $cm^{-2}$ was obtained during PEC experiment without any external voltage under chopped light irradiation (1 sun, 50 min on, 10 min off, **Figure 3b**). After 10 h, syngas was detected in the cathode with 54.6±9.2 μmol $cm^{-2}$ CO and 106.6±8.4 μmol $cm^{-2}$ $H_2$ ($FE_{CO}$ 34.1±2.2% and $FE_{H2}$ 70.3±1.8%, **Figure 3c**). The turnover number of the molecular catalyst for CO formation ($TON_{CO}$) was estimated 3657±591 (**Figure 3d**). No other reduction products were detected in NMR spectroscopic analysis of the catholyte. The high performance liquid chromatography (HPLC) analysis of the anolyte showed GA as only oxidation product with 85.8±16.2 μmol $cm^{-2}$ yield ($FE_{GA}$ 92.5±5.3%). The possibility of employing real-world PET waste as EG precursor was confirmed by using alkaline pre-treated commercial PET plastic bottle solution as anolyte (~0.2 M EG, see methods), which showed similar yields and FE for $H_2$, CO, and GA formation after 10 h of PEC experiment without external voltage (**Figure S19**).

CV scans of $CO_2$ captured in NaOH/EG electrolyte under solar-irradiation also showed an onset voltage around –0.4 V (**Figure 3e)** with j ~0.35 mA $cm^{-2}$ at zero applied voltage. The steady state photocurrent density was 0.18±0.07 mA $cm^{-2}$ over 10 h PEC experiment without external voltage (**Figure 3f**). After 10 h, 5.2±1.1 μmol $cm^{-2}$ CO and 16.4±0.6 μmol $cm^{-2}$ $H_2$ were produced ($FE_{CO}$ 18.2±1.1%, $FE_{H2}$ 58.2±4.0%) with total syngas FE ~76% and $TON_{CO}$ of 347±74 (**Figures 3g-3h)**. No other reduction products (e.g., formate, methanol) were detected in $^1$H-NMR analysis. The amount of GA was 11.7±3.5 μmol $cm^{-2}$ ($FE_{GA}$ ~86±11%, **Figure 3f**), as the only detected oxidation product at anode by HPLC analysis.

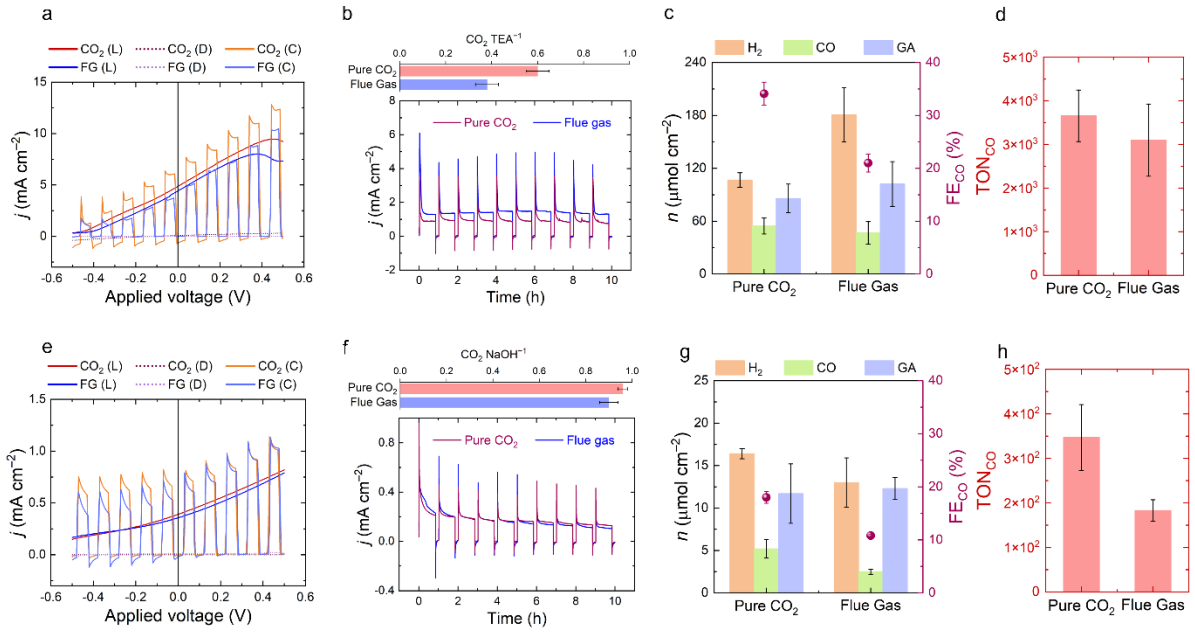


**Figure 3. Photoelectrochemical conversion of captured $CO_2$.** Photoelectrochemical (PEC) response of TEA/$H_2O$ system: **a**, Representative forward linear sweep voltammetry (LSV) scans (scan rate 10 mV $s^{-1}$) recorded with the PVK|$CoPcNH_2$@MWCNT photocathode under continuous (L: Light), chopped (C: Chopped, 5s on, 5s off), or no (D: Dark) simulated solar light irradiation (1 sun, 100 mW $cm^{-2}$, AM 1.5G) for $CO_2$ captured from pure concentrated stock and flue gas in a two-compartment two-electrode PEC configuration (catholyte, capture solution with 0.1 M added $K_2SO_4$; anolyte, 0.5 M KOH, 0.5 M EG in water; photocathode: PVK|$CoPcNH_2$@MWCNT; anode: Ni foam|$Cu_{26}Pd_{74}$; bipolar membrane). **b**, Corresponding photocurrent transients for 10 h (without any external applied voltage) operation under 1 sun chopped irradiation (50 min on, 10 min off) for $CO_2$ captured TEA/$H_2O$ solution with pure $CO_2$ (red) and flue gas (blue). The amounts of captured $CO_2$ in the solution are shown on top. **c**, Product distribution from both anode and cathode sides after 10 h of PEC reaction and the observed $FE_{CO}$ values. **d**, Obtained turnover numbers (TON) for CO formation. PEC response of NaOH/EG system: **e**, Representative forward LSV scans (scan rate 10 mV $s^{-1}$) recorded with the PVK|$CoPcNH_2$@MWCNT photocathode in NaOH/EG system. **f**, Photocurrent transient obtained during 10 h PEC experiments under 1 sun chopped irradiation (50 min on, 10 min off) with $CO_2$ captured NaOH/EG solution with concentrated $CO_2$ and flue gas without any external applied voltage. **g**, Cathodic and anodic product distribution after 10 h of PEC reaction with the observed $FE_{CO}$ values, and **h,** the TONs obtained (catholyte, capture solution with added 20% v/v MeCN and 0.15 M $TBABF_4$ electrolyte; anolyte, 0.6 M NaOH, 0.15 M $TBABF_4$ in 20% (v/v) MeCN in EG; photocathode, PVK|$CoPcNH_2$@MWCNT; anode, Ni foam|$Cu_{26}Pd_{74}$; bipolar membrane). All experiments were carried out at room temperature.

## Solar-driven conversion of flue gas captured $CO_2$

Real-world implications of our developed integrated CCU system was investigated using simulated post-combustion flue gas as $CO_2$ source. Industrial flue gas typically contains ~15% $CO_2$, 3-5% $O_2$ and $N_2$ gas with some $SO_x$ and $NO_x$ impurities which can be minimized by wet-scrubbing.[38,39] Our simulated flue gas contained only major components: $CO_2$ (15%), $O_2$ (4%), and $N_2$ (81%).[40,41] The capture was done by purging simulated flue gas through capture solutions (1 M TEA/$H_2O$ or NaOH/EG) for 6 h at 30 mL $min^{-1}$ flowrate. $^{13}$C-NMR analysis showed that after 6 h, TEA/$H_2O$ captured 0.38±0.05 mol $CO_2$ per mol TEA (as bicarbonate salt), and the

NaOH/EG solution captured 0.90±0.04 mol $CO_2$ per mol NaOH as sodium glycolate carbonate. Electrochemical CPE of the post-capture solutions with $CoPcNH_2$@MWCNT cathode at optimized potentials (–0.7 V vs. RHE or –1.85 V vs. $Fc/Fc^+$) showed syngas production with $FE_{CO}$ 24.0±0.9% and 11.9±0.3% in the TEA/$H_2O$ and NaOH/EG medium, respectively (**Figure S20**). Subsequent solar-driven PEC conversion of captured $CO_2$ from flue gas was performed with the PVK|$CoPCNH_2$@MWCNT photocathode in a two-electrode configuration without external voltage. CVs recorded under solar irradiation showed an onset at –0.4 V in both TEA/$H_2O$ and NaOH/EG medium with respective photocurrent densities of ~5 mA $cm^{-2}$ and ~0.4 mA $cm^{-2}$ at zero applied voltage (**Figures 3a, 3e**). Steady-state photocurrent densities of 1.3±0.4 mA $cm^{-2}$ and 0.18±0.07 mA $cm^{-2}$ were observed during the PEC experiment in respective media (**Figures 3b, 3f**). After 10 h of solar irradiation (with no applied voltage) TEA/$H_2O$ system produced 46.8±12.7 μmol $cm^{-2}$ CO ($FE_{CO}$ 21.0±1.7, $TON_{CO}$ 3098±827) and 180.7±30.6 μmol $cm^{-2}$ $H_2$ ($FE_{H2}$ 81.1±3.2%) (**Figures 3c-d**). Similarly, the NaOH/EG system produced 2.5±0.3 μmol $cm^{-2}$ CO ($FE_{CO}$ 10.8±0.2%, $TON_{CO}$ 183±24) and 13.0±2.9 μmol $cm^{-2}$ $H_2$ ($FE_{H2}$ 52.0±5.0%) after 10 h PEC experiment (**Figures 3g-h**). HPLC analysis of the anolyte showed 102.2±25.4 μmol $cm^{-2}$ GA ($FE_{GA}$ 89.4±5.2%) for TEA/$H_2O$ medium and 12.3±1.3 μmol $cm^{-2}$ GA ($FE_{GA}$ 93.7±1.0%) for NaOH/EG medium **(Figures 3c and 3g**), suggesting completion of both flue gas captured $CO_2$ reduction and plastic derived EG oxidation.

**Direct air capture and solar-driven conversion**

The solar-driven conversion of atmospheric $CO_2$ was further investigated. Direct air capture (DAC) of $CO_2$ and its conversion into value-added products is a promising technology to afford an overall negative carbon footprint when conversion is done with a renewable energy source such as sunlight. Moreover, DAC technologies can be easily decentralized to desired locations, opposed to capture from concentrated point sources requiring proximity to emissions. The direct capture and conversion of aerobic $CO_2$ is especially challenging due to the ultra-low concentration, requiring aggressive capturing agents for suitable kinetics and consequently higher thermodynamic input for chemical reduction. We performed the atmospheric $CO_2$ capture by pumping indoor air through capture solutions (1 M aqueous TEA or glycolic NaOH) at 1.8 L $min^{-1}$ flowrate for 2 days using an aquarium pump (**Figure 4a**). The TEA/$H_2O$ solution captured only 0.02±0.01 mol $CO_2$ per mol TEA after this time due to slow capture kinetics. In contrast, capture efficiency of the NaOH/EG solution was notable reaching 0.73±0.07 mol of captured $CO_2$ per mol NaOH (**Figures 4a-b**).

Electrochemical reduction of TEA captured atmospheric $CO_2$ at –0.7 V vs. RHE with $CoPcNH_2$@MWCNT cathode produced negligible CO due to very low captured $CO_2$ availability. Contrarily, CPE of the atmospheric $CO_2$ captured in NaOH/EG solution at –1.85 V vs $Fc/Fc^+$ produced CO with 2.9±0.3% FE, showing electrochemical conversion of direct air captured $CO_2$ (**Figure S21**). We note that despite a modest captured $CO_2$ concentration (0.73 M), the $FE_{CO}$ is lower compared to $CO_2$ captured from a pure stream ($FE_{CO}$ ~20%). This is likely due to the incomplete $CO_2$ capture (owing to equilibrium shift in ultra-low $CO_2$ concentration as per Le Chatelier's principle), which leads to higher alkalinity of the post-capture medium and a more challenging conversion process (supplemental discussion, **Figure S22**).[42]

Solar-driven PEC reduction of captured atmospheric $CO_2$ in TEA solution with PVK|$CoPcNH_2$@MWCNT photocathode did not produce any CO. In contrast, the organic NaOH/EG medium was more suitable for the solar-driven conversion of atmospheric $CO_2$. PEC experiment with $CO_2$ captured in glycolic NaOH solution after DAC produced 2.1±0.5 μmol

$cm^{-2}$ CO after 110 h under 1 sun irradiation with no applied voltage (**Figures 4c-d**). The CO production rate remained consistent over the reaction period with final $FE_{CO}$ and $TON_{CO}$ reaching 2.3±0.4% and 141±38, respectively (**Figure 4e**). A control experiment without DAC produced tiny amount of CO due to epoxy degradation in EG medium, that was subtracted for all atmospheric $CO_2$ conversion calculations (**Figure S23**).[43,44] HPLC analysis of the anolyte showed 61.6±8.3 µmol $cm^{-2}$ GA formation ($FE_{GA}$ 85.7±2.2%) that indicates the completion of overall PEC process. While further optimization is necessary to improve the overall CO formation efficiency, this proof-of-concept study demonstrates the viability of direct long-term solar-driven reduction of atmospheric $CO_2$ to CO following DAC, using perovskite-PEC systems. Future work in this regard would benefit from the use of solar cells with higher $V_{OC}$ to match the stringent thermodynamic demands of air captured $CO_2$ conversion.

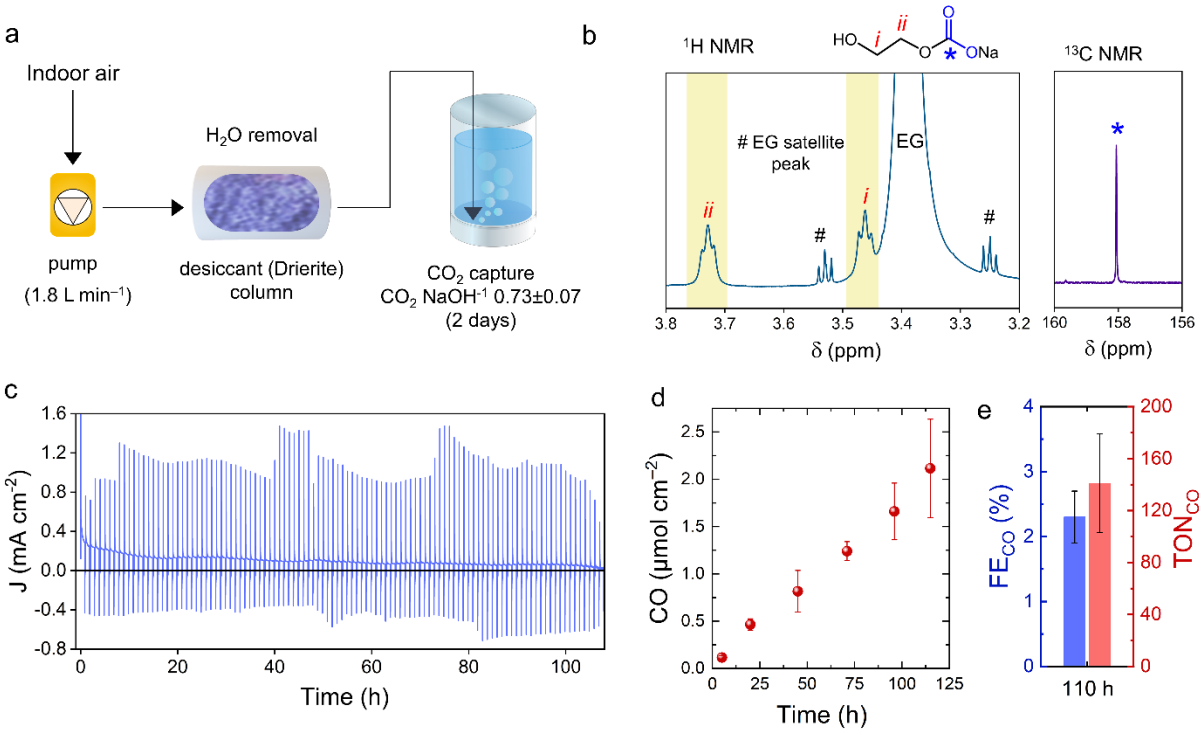


**Figure 4. PEC conversion of atmospheric $CO_2$.** **a**, Schematic diagram of the setup showing the capture process in glycolic NaOH medium. $CO_2$ capture was performed by pumping indoor air through a 1M NaOH solution in EG for 2 days (flowrate 1.8 L $min^{-1}$; capture amount: 0.73±0.07 mol $CO_2$ per mol /$OH^-$). **b**, $^1H$ and $^{13}C$ NMR of the post capture solution showing the capture products. **c**, PEC reduction of post DAC solution: photocurrent transient for 110 h PEC experiment under simulated solar irradiation with no applied external voltage. The unusually long spikes are because of charge recombination owing to the low availability of reducing species ($CO_2$ or proton) in the medium. **d**, Production of CO with time which remained almost linear with progress of experiment demonstrating the longevity of the system. **e**, Corresponding $FE_{CO}$ and $TON_{CO}$ after 110 h PEC experiment. Conditions- Catholyte, capture solution with added 20% v/v MeCN and 0.15 M $TBABF_4$; anolyte, 0.6 M NaOH, 0.15 M $TBABF_4$ in 20% v/v MeCN in EG; photocathode, PVK|$CoPcNH_2$@MWCNT; anode, Ni foam|$Cu_{26}Pd_{74}$; bipolar membrane; 1 sun chopped irradiation (AM1.5G, 50 min on, 10 min off); room temperature.

## Conclusions

This work demonstrates capture and direct solar-driven utilization of $CO_2$ to syngas, in combination with plastic-derived waste oxidation, in a two-compartment PEC setup. $CO_2$ is captured from a concentrated stream or simulated flue gas or air in amine/hydroxide solution, and directly converted over a PVK|$CoPcNH_2$@MWCNT photocathode under 1 sun irradiation. A Ni foam|$Cu_{26}Pd_{74}$ alloy anode completes the circuit by catalyzing EG oxidation to GA selectively. Replacing thermodynamically challenging water oxidation with EG oxidation allows the system to operate with a single light absorber without any externally applied voltage. Real-world plastic waste can be directly used as EG source after alkaline pre-treatment, facilitating waste valorization. Utilizing air as the $CO_2$ source, pre-treated waste plastics as electron donors, and sunlight as the energy source, this proof-of-concept $CO_2$ capture and solar-driven utilization system could be promising for future decentralized off-the-grid scalable solar fuels and chemical synthesis.

## METHODS

### *Materials*

Triethanolamine (TEA, ≥99%, Sigma-Aldrich), monoethanolamine (MEA, ≥99%, Sigma-Aldrich), diethanolamine (DEA, ≥99%, Sigma-Aldrich), 1,4-diazabicyclo[2.2.2]octane (DABCO, ≥99%, Sigma-Aldrich), sodium hydroxide (NaOH, ≥99.99% semiconductor grade, Sigma-Aldrich), potassium hydroxide (KOH, ≥99.99% semiconductor grade, Sigma-Aldrich), ethylene glycol (≥99%, Sigma-Aldrich), cobalt(II) 2,9,16,23-tetra(nitro)phthalocyanine ($CoPcNO_2$, >95%, PorphyChem), sodium sulfide nonahydrate ($Na_2S.9H_2O$, ≥99.99% trace metals basis, Sigma-Aldrich), nickel foam (1.6 mm thickness, MJ group), sulfuric acid (Suprapur 96%, Merck), FTO-coated glass (≈7Ω $sq^{-1}$, 2.2 mm thick, Sigma-Aldrich), Zn (dust, 98+%, ACROS), hydrogen peroxide ($H_2O_2$, 30% w/v, Fisher Scientific), hydrochloric acid (HCl, fuming, 36.5–38%, Honeywell), nickel nitrate hexahydrate ($Ni(NO_3)_2{\cdot}6H_2O$, ≥98.5%, Sigma-Aldrich), ethylenediamine (absolute, ≥99.5%, Fluka), lead iodide ($PbI_2$, 99.99%, trace metals basis, TCI), lead bromide ($PbBr_2$, for perovskite precursor, TCI), *N*,*N*-dimethylformamide (DMF, anhydrous, 99.8%, Sigma-Aldrich), dimethyl sulfoxide (DMSO, anhydrous, ≥99.9%, Sigma-Aldrich), formamidinium iodide (Dyesol), methylammonium bromide (Dyesol, 1-methyl-2-pyrrolidone (99.5%, extra dry over molecular sieves, ACROS), dimethyl sulfoxide (ACS reagent, ≥99.9%), chloroform (99.9%, extra dry over molecular sieves, stabilized, ACROS), PCBM (99%, Solenne BV), chlorobenzene (extra dry over molecular sieves ≥99.5%, ACROS) polyethyleneimine (PEIE, 80% ethoxylated solution, 35–40 wt% in $H_2O$, average $M_w$ 70 000, Sigma-Aldrich), 2-propanol (≥99.5%, Honeywell), poly[bis(4-phenyl)(2,4,6-trimethylphenyl)amine (PTAA, $M_w$ 17700, EM INDEX), 2,3,5,6-Tetrafluoro-7,7,8,8-tetracyanoquinodimethane (F4TCNQ, 97%, Sigma-Aldrich), graphite powder (20 µm, Sigma-Aldrich), Araldite 5-Minute Rapid two component epoxy, Araldite Standard two component epoxy, Nafion™ solution (5 wt.% v/v in lower aliphatic alcohols and water, Sigma-Aldrich), potassium sulphate ($K_2SO_4$, 99.99%, Sigma-Aldrich), sodium carbonate ($Na_2CO_3$, ≥99.5%%, Sigma-Aldrich), tetrabutylammonium tetrafluoroborate ($TBABF_4$, ≥99.0% for electrochemical analysis, Sigma-Aldrich), acetonitrile (MeCN, anhydrous 99.8%, Sigma-Aldrich), carbon dioxide (99.995% CP grade, BOC), simulated flue gas (4% $O_2$, 15% $CO_2$,

Nitrogen 200 bar, BOC), carbon-$^{13}$C dioxide ($^{13}CO_2$, 99.0 atom% $^{13}$C, Sigma-Aldrich) were used without further purification unless otherwise stated.

***Synthesis of $CoPcNH_2$ molecular catalyst and assembly of $CoPcNH_2$@MWCNT***

$CoPcNH_2$ was synthesized by slightly modifying a previously reported procedure.[31] In short, crude $CoPcNO_2$ (0.61 g, 0.82 mmol) was dissolved in DMF (10 mL) and $N_2$ purged for 15 min. Sodium sulphide (60 wt% $Na_2S \cdot xH_2O$) (2.1 g) was added to the mixture under nitrogen and dark green solution was heated at 80 °C. After cooling to room temperature, the reaction mixture was poured over 150 mL ice cold water. The green product was collected by filtration and washed with water, 20 mL EtOH (until colourless), and diethyl ether to give $CoPcNH_2$ with 0.5 g yield (80%). The complex was characterized by ATR-IR (1750, 1680, 1607, 1458 $cm^{-1}$), UV-vis (Q-band $\lambda_{max}$ 704 nm ($\varepsilon$= $4.1x10^4$ $M^{-1}$ $cm^{-1}$, DMSO), and elemental analysis Calculated ($C_{32}H_{20}CoN_{12}$): C 60.86; H 3.19; N 26.62; Found: C 59.25, H 3.72, N 26.14 (probable fitting, $C_{32}H_{20}CoN_{12} + H_2O$; calculated: C 59.17, H 3.41, N 25.88).

To prepare the electrodes, MWCNT (5 mg) was dispersed in DMF (2.34 mL) using a probe sonicator for 20 min. Then, 600 μL of freshly made $CoPcNH_2$ solution in DMF (1 mM) and of Nafion$^{TM}$ (60 μL, 5 % v/v in lower aliphatic alcohols and water) were added to the dispersion. The mixture was sonicated for an additional 15 min. 100 μL of this catalyst ink was then drop-casted over an activated graphite foil substrate (active area ~0.84 $cm^2$). The ink was allowed to dry for a minimum two days at room temperature. The fabricated catalyst is denoted as $CoPcNH_2$@MWCNT and characterised by SEM, SEM-EDX, ICP-OES analysis.

***Preparation of PVK|$CoPcNH_2$@MWCNT photocathodes***

The inverse structure triple cation mixed halide perovskite devices were prepared following a previously reported procedure.[33] In brief, a hole transporting layer (HTL) of $NiO_x$ was first deposited on a FTO collated glass substrate by spin coating a solution of $Ni(NO_3)\cdot 6H_2O$ (1 M), and ethylenediamine in EG (1 M), and was then annealed at 373 K for 30 min. A second hole transporting layer was deposited over the $NiO_x$ by spin coating a F4TCNQ doped PTAA solution inside a $N_2$ filled glove box. A perovskite layer was then deposited on top of the HTLs. For this purpose, a cesium formamidinium methylammonium (CsFAMA) perovskite precursor solution was first prepared by adding a solution of $FAMA_{0.22}Pb_{1.32}I_{3.2}Br_{0.66}$ (1000 μL) to DMF (510 μL), DMSO (340 μL) and 1-methyl-2-pyrrolidone (150 μL), and then adding CsI in DMSO (1.5 M, 48 μL). The perovskite layer was then deposited over the PTAA layer using a two-step spin coating process, first for 10 s at 1000 rpm, followed by 35 s at 6000 rpm. Chloroform was used as the antisolvent for the final 7 sec before the end. Afterwards, the PVK layer was annealed at 373 K for 30 min. Subsequently, a [6,6]-phenyl C61 butyric acid methyl ester (PCBM; 35 mg $mL^{-1}$ in chlorobenzene) solution was spin coated on top of the perovskite layer at 3000 rpm for 45 sec as an electron transport layer (ETL). A PEIE film layer was then deposited over the PCBM coated perovskite device using a precursor solution (3.9 μL $mL^{-1}$ solution in isopropanol), which helps in stopping the interfacial degradation. Finally, a 100 nm conductive Ag layer was deposited over the PEIE layer using metal evaporation technique through a patterned mask, ensuring an active perovskite surface area of ~0.5 x 0.5 $cm^2$.

The perovskite devices were interfaced with the $CoPcNH_2$@MWCNT catalyst to prepare the photocathode, which were subsequently encapsulated with epoxy to stop their degradation inside aqueous medium. For interfacing the devices with the catalyst, a conductive graphite epoxy (GE) paste was prepared by homogeneously mixing graphite powder with epoxy in 3:4

mass ratio.[33,34] Araldite standard two-part epoxy was used for this purpose. The paste was then applied evenly over the Ag contact layer of the perovskite device, on top of which the graphite foil containing the $CoPcNH_2$@MWCNT catalyst was attached. The device was then left to dry for 24 h to harden the GE layer, after which a Cu wire was attached for connection. Finally, the assembled device was encapsulated, and the edges were sealed using Araldite 5-min Rapid 2 component epoxy. The final PVK-based photocathodes are referred to as PVK|$CoPcNH_2$@MWCNT.

***Synthesis of the $Cu_{26}Pd_{74}$ oxidation catalyst***

The $Cu_{26}Pd_{74}$ oxidation catalyst was synthesized by a dynamic $H_2$ bubble template assisted galvanostatic electrodeposition method using an activated Ni foam as scaffold.[5,45] The electrodeposition was carried out in a single compartment three-electrode configuration, where a leakless double junction Ag/AgCl electrode (sat. KCl, Metrohm, Switzerland) was used as a reference electrode, an activated Ni foam scaffold was used as the working electrode, and a Pt foil (~6 $cm^2$ area) was used as the counter electrode. The electrolyte solution contained a total 0.02 M solution of $CuSO_4 \cdot 5H_2O$ and $Na_2PdCl_4$ salts with a $Cu^{2+}$:$Pd^{2+}$ molar ratio of 30:70. The galvanostatic electrodeposition was carried out by applying a current density of $-2$ A $cm^{-2}$ for 40 s. The formed bimetallic catalyst was then washed with Milli Q® water multiple times to remove any residual salt and acid and was subsequently dried under $N_2$ flow.

***Material characterization***

The FESEM images were acquired using TESCAN MIRA3 FEG-SEM instrument equipped with an Oxford Instruments Aztec Energy X-maxN 80 EDX system. The UV-vis spectra were recorded using a Varian Cary 50 UV-vis spectrophotometer. The ICP-OES measurements were performed on a Thermo Scientific iCAP 7400 ICP-OES DUO spectrometer at the Microanalysis Service, Yusuf Hamied Department of Chemistry, University of Cambridge.

***$CO_2$ capture experiments***

The $CO_2$ capture form concentrated $CO_2$, flue gas and ambient air was carried out by bubbling the respective $CO_2$ containing gas through a capture solution. Briefly, the capture solution was prepared by dissolving the amine/hydroxide in water/ethylene glycol solvent to make a concentration of 1 M. Concentrated $CO_2$ or simulated flue gas (15% $CO_2$, 4% $O_2$, balance $N_2$) was then bubbled through the solution at 30 mL $min^{-1}$ for 2 h or 6 h, respectively (**Figure S2**). For $CO_2$ capture from air, indoor air (Reisner Lab, Yusuf Hamied Department of Chemistry, University of Cambridge) was pumped through the capture solution at a flow rate of 1.8 L $min^{-1}$ after passing it through a Drierite® column for drying, using a Pawfly Ultra Quiet Air Pump (MA-60) (**Figure 4a**). Afterwards, the capture solutions were purged with $N_2$ for 15 mins to remove any physically dissolved $CO_2$ or $O_2$. 0.5 mL of the solution was analysed by $^1H$ and $^{13}C$ NMR spectroscopy, after addition of 1,4-dioxane (aqueous systems) or imidazole (organic systems) as internal standard and $D_2O$ (aqueous)/DMSO-$d_6$ (organic) as the deuterated solvent to characterize and quantify the captured products. The remaining solution was used as $CO_2$ source for the electrochemical and PEC studies after addition of supporting electrolytes/solvents as previously mentioned.

***Electrochemical and PEC measurements***

The electrochemical measurements were carried out with a PalmSens Muti EmStat3+ potentiostat, whereas the PEC measurements were carried out with a Ivium CompactStat potentiostat and a Newport Oriel 67005 solar light simulator equipped with an Air Mass 1.5 Global (AM 1.5G) solar filter. All experiments were carried out in a two compartment H cell separated by a bipolar membrane in reverse bias. For the electrochemical experiments in the aqueous system, the catholyte typically consisted of the capture solution (resulting from $CO_2$ capture from pure $CO_2$ or flue gas or air as previously described) with added 0.1 M $K_2SO_4$ and the14oluteion was purged with $N_2$ containing 2% $CH_4$ as an internal standard for 15 min. The anolyte consisted of 0.1 M $K_2SO_4$ purged with $N_2$ containing 2% $CH_4$ for 15 min, with the working, counter and the reference electrodes being $CoPcNH_2$@MWCNT, Pt mesh, and an Ag/AgCl (sat. NaCl) electrode, respectively. For the glycolic capture solutions, the catholyte typically consisted of the capture solution with added 20% v/v MeCN co-solvent and 0.15 M $TBABF_4$ supporting electrolyte, whereas the anolyte was 0.6 M NaOH, 0.15 M $TBABF_4$ in 20% v/v MeCN in EG solvent mixture (both catholyte and anolyte were purged with $N_2$ containing 2% $CH_4$ for 15 min prior to experiment), and the working, counter and reference electrodes were $CoPcNH_2$@MWCNT, Ni foam|$Cu_{26}Pd_{74}$ and Ag/$AgNO_3$ (in 0.1 M *n*-$Bu_4NPF_6$ in MeCN) electrode, respectively. The potentials recorded with the Ag/AgCl (sat. NaCl) and Ag/$AgNO_3$ (in 0.1 M *n*-Bu4$NPF_6$ in MeCN) reference electrodes were converted to the RHE and $Fc/Fc^+$ scales, respectively, as per following equations:

$$E_{(RHE)} = E_{(Ag/AgCl)} + 0.197\,V + 0.059 \times pH \quad (5)$$

$$E_{(Fc/Fc+)} = E_{(Ag/AgNO3)} + 0.41\,V \quad (6)$$

The $E_{1/2}$ of the $Fc/Fc^+$ couple was determined as 0.41 V vs. Ag/$AgNO_3$ (in 0.1 M *n*-$Bu_4NPF_6$ in MeCN) by cyclic voltammetry (50 mV $s^{-1}$) in a single compartment three-electrode configuration with glassy carbon as the working electrode, Pt mesh as the counter electrode and Ag/$AgNO_3$ (in 0.1 M *n*-$Bu_4NPF_6$ in MeCN) as the reference electrode, using an electrolyte containing 5 mM ferrocene and 0.15 M $TBABF_4$ in 20% v/v MeCN in EG media.

The dark CV scans for the Ni foam|$Cu_{26}Pd_{74}$ were taken in a three electrode two-compartment setup with Pt mesh as the counter electrode and Ag/AgCl (sat. NaCl) or Ag/$AgNO_3$ (in 0.1 M *n*-$Bu_4NPF_6$ in MeCN) as the reference electrode for aqueous and glycolic systems, respectively (scan rate 10 mV $s^{-1}$). Similarly, the CV scans of the assembled photocathode (PVK|$CoPcNH_2$@MWCNT) were recorded in a three-electrode system in both aqueous TEA captured and glycolic NaOH captured $CO_2$ medium under chopped (5 s on, 5 s off), continuous or no simulated solar illumination (1 sun), with Ni foam|$Cu_{26}Pd_{74}$ counter electrode, and Ag/AgCl (sat. NaCl) or Ag/$AgNO_3$ (in 0.1 M *n*-$Bu_4NPF_6$ in MeCN) as the reference electrode for aqueous and glycolic systems, respectively, at a scan rate of 10 mV $s^{-1}$. The Newport Oriel 67005 solar light simulator was calibrated to 1 sun (100 mW $cm^{-2}$) using a Newport light meter before each experiment. The working potentials of both cathode and anodes under solar illumination (without any external voltage) were determined from CV overlaps.

The two-electrode two-compartment PEC experiments were carried out with PVK|$CoPcNH_2$@MWCNT photocathode and Ni foam|$Cu_{26}Pd_{74}$ as the dark anode, where captured $CO_2$ conversion to syngas and EG oxidation to GA were performed simultaneously under 1 sun solar irradiation without applying any external voltage. The catholytes were capture solution + 0.1 M $K_2SO_4$ (aqueous medium) or capture solution + 20% v/v MeCN + 0.15 M $TBABF_4$ (organic medium), and the anolytes were 0.5 M KOH, 0.5 EG in water (aqueous

medium) or 0.6 M NaOH, 0.15 M $TBABF_4$ in 80/20 v/v EG/MeCN solvent mixture (organic medium). CV scans in this two-electrode configuration were recorded at 10 mV $s^{-1}$ scan rate to observe the photoelectrochemical response under chopped, continuous, and no light irradiation. The PEC experiments were carried out under chopped irradiation (50 min on, 10 min off) at no applied voltage for a certain time period, and the obtained photocurrents were normalized to the perovskite active area. Product analysis and quantification was carried out after each PEC experiment.

For the isotopic labelling experiments with $^{13}CO_2$, the $^{13}CO_2$ capture was performed by stirring the 1 M TEA solution in water or 1 M NaOH solution in EG for 2 h under $^{13}CO_2$ atmosphere. The obtained solutions were purged with $N_2$ for 15 min to remove physically dissolved $^{13}CO_2$ and were then used for electrochemical reduction as per standard electrochemical conditions. The product gas mixture generated in the cathode after 2 h (at –0.7 V vs. RHE, TEA/$H_2O$ system) or 20 h (at –1.85 V vs. $Fc/Fc^+$, NaOH/EG system) of CPE were analysed by IR spectroscopy to determine the isotopic abundance in the product CO.

For the experiment with real-world waste PET plastic derived EG, a commercial sparkling water PET bottle (Highland Spring, sourced from Sainsbury's UK) was pre-treated with alkaline pre-treatment.[5] The bottle was cut in small pieces, dipped in liquid $N_2$ and then pulverized in a grinder. 1 M aqueous KOH was then added (PET concentration 50 mg $mL^{-1}$) and the solution was heated at 80 ºC for 5 days under continuous stirring. The solution was then filtered to remove PET fragments and the clear solution was directly used as anolyte for the PEC experiments. The concentration of EG after pre-treatment was determined as 10.3±2.8 mg $mL^{-1}$ (~0.2 M) by HPLC.

***Product detection and quantification***

The gases $H_2$ and CO produced at the cathode were detected and quantified using a Shimadzu GC-2010 Plus gas chromatogram with ultrapure Helium as the carrier gas. 2% $CH_4$ in the purging $N_2$ gas after $CO_2$ capture was used as an internal standard for quantification. Gaseous aliquots were taken from the headspace and were analysed by manual injection to the GC. The liquid aliquots from both cathodic and anodic compartments were taken after the experiments, and then analysed by $^1H$ NMR spectroscopy or HPLC. A Waters breeze HPLC system equipped with a Phenomenex Rezex 8% $H^+$ column and refractive index (RIS-2414) and diode array UV-Vis (254 nm) detectors was used for the oxidation product quantification. The faradic efficiencies (FE) of products were determined from equation 7,

$$\mathrm{FE[product]}\ (\%) = \frac{Z n F}{Q_{passed}} \times 100 \qquad (7)$$

where Z is the number of electrons required for the respective product formation, n is the number of moles of product formed, F is the Faraday constant (96485 C $mol^{-1}$) and $Q_{passed}$ is the total amount of change passed during experiment.

The turnover number (TON) of the molecular catalyst was calculated as per the following equation:

$$\mathrm{TON} = \frac{moles\ of\ product\ formed}{moles\ of\ catalyst} \qquad (8)$$

For isotopic labelling experiments with $^{13}CO_2$, the isotopic abundance of the generated product CO was recorded in a Thermo Scientific Nicolet iS50 IR spectrometer in a gas-phase

transmission mode. The generated gas mixture after the experiment was transferred from the cathode headspace by vacuum extraction to an IR cell equipped with KBr windows with 10 cm path length.

## DATA AVAILABILITY

The raw data that support the findings of this study will be available from the University of Cambridge data repository (DOI to be added after acceptance of the manuscript).

## ACKNOWLEDGEMENTS

This work was supported by the Sustainability and Energy Research Initiative (SAERI) research fellowship of Weizmann Institute of Science (to S.K.), UKRI Engineering and Physical Sciences Research Council (Grant Ref: EP/X023370/1 to S.K.), the European Commission Marie Sklodowska-Curie Individual European Fellowships (GAN 839763 to M.R. and GAN 745604 to S.R.), the Cambridge Trust (Vice-Chancellor's Award to V.A. and HRH The Prince of Wales Commonwealth Scholarship to S.B.), the Winton Programme for the Physics of Sustainability and St John's College (Title A Research Fellowship to V.A.), the UKRI Cambridge Circular Plastics Centre (CirPlas, EP/S025308/1 to E.R.) and the Hermann and Marianne Straniak Stiftung (to E.R.). The authors acknowledge Dr. Heather Greer for the assistance with microscopy analysis, Dr. Peter Gierth, Mr. Duncan Howe, and Mr. Andrew Mason for assistance with NMR measurements, and Dr. Tessel Bouwens, Dr Yongpeng Liu (Department of Chemistry, University of Cambridge) for useful feedback on the manuscript

## AUTHOR CONTRIBUTIONS

S.K., M.R., and E.R. designed the project. S.K. and M.R. fabricated the (photo)electrodes and carried out all the capture and PEC experiments. V.A. prepared and characterized the perovskite devices. S.B. assisted with PEC, HPLC measurements and schematic diagrams. S.R. synthesized the molecular $CO_2$ reduction catalyst. S.K., M.R., and E.R. collectively wrote the manuscript with the help of all co-authors. E.R. supervised the work.

## COMPETING INTERESTS

The authors declare no competing financial interest.

## REFERENCES

1. Hannah Ritchie, Max Roser and Pablo Rosado (2020) - "$CO_2$ and Greenhouse Gas Emissions". Published online at OurWorldInData.org. Retrieved from: 'https://ourworldindata.org/co2-and-other-greenhouse-gas-emissions' [Online Resource]
2. IEA (2020), CCUS in Clean Energy Transitions, IEA, Paris https://www.iea.org/reports/ccus-in-clean-energy-transitions

3. Creissen, C.E., and Fontecave, M. (2021). Solar-Driven Electrochemical $CO_2$ Reduction with Heterogeneous Catalysts. Adv. Energy Mater. *11*, 2002652. https://doi.org/10.1002/aenm.202002652.
4. Morikawa, T., Sato, S., Sekizawa, K., Suzuki, T.M., and Arai, T. (2022). Solar-Driven $CO_2$ Reduction Using a Semiconductor/Molecule Hybrid Photosystem: From Photocatalysts to a Monolithic Artificial Leaf. Acc. Chem. Res. *55*, 933-943. 10.1021/acs.accounts.1c00564.
5. Bhattacharjee, S., Andrei, V., Pornrungroj, C., Rahaman, M., Pichler, C.M., and Reisner, E. (2022). Reforming of Soluble Biomass and Plastic Derived Waste Using a Bias-Free $Cu_{30}Pd_{70}$|Perovskite|Pt Photoelectrochemical Device. Adv. Funct. Mater. *32*, 2109313. https://doi.org/10.1002/adfm.202109313.
6. Sanz-Pérez, E.S., Murdock, C.R., Didas, S.A., and Jones, C.W. (2016). Direct Capture of $CO_2$ from Ambient Air. Chem. Rev. *116*, 11840-11876. 10.1021/acs.chemrev.6b00173.
7. McQueen, N., Gomes, K.V., McCormick, C., Blumanthal, K., Pisciotta, M., and Wilcox, J. (2021). A review of direct air capture (DAC): scaling up commercial technologies and innovating for the future. Prog. Energy *3*, 032001. 10.1088/2516-1083/abf1ce.
8. Rochelle, G.T. (2009). Amine Scrubbing for $CO_2$ Capture. Science *325*, 1652-1654. doi:10.1126/science.1176731.
9. Wu, X., Yu, Y., Qin, Z., and Zhang, Z. (2014). The Advances of Post-combustion $CO_2$ Capture with Chemical Solvents: Review and Guidelines. Energy Procedia *63*, 1339-1346. https://doi.org/10.1016/j.egypro.2014.11.143.
10. Sullivan, I., Goryachev, A., Digdaya, I.A., Li, X., Atwater, H.A., Vermaas, D.A., and Xiang, C. (2021). Coupling electrochemical $CO_2$ conversion with $CO_2$ capture. Nat. Catal. *4*, 952-958. 10.1038/s41929-021-00699-7.
11. Heldebrant, D.J., Kothandaraman, J., Dowell, N.M., and Brickett, L. (2022). Next steps for solvent-based $CO_2$ capture; integration of capture, conversion, and mineralisation. Chem. Sci. *13*, 6445-6456. 10.1039/D2SC00220E.
12. Kar, S., Goeppert, A., and Prakash, G.K.S. (2019). Integrated $CO_2$ Capture and Conversion to Formate and Methanol: Connecting Two Threads. Acc. Chem. Res. *52*, 2892-2903. 10.1021/acs.accounts.9b00324.
13. Jerng, S.E., and Gallant, B.M. (2022). Electrochemical reduction of $CO_2$ in the captured state using aqueous or nonaqueous amines. iScience *25*, 104558. https://doi.org/10.1016/j.isci.2022.104558.
14. Kothandaraman, J., Goeppert, A., Czaun, M., Olah, G.A., and Prakash, G.K.S. (2016). Conversion of $CO_2$ from Air into Methanol Using a Polyamine and a Homogeneous Ruthenium Catalyst. J. Am. Chem. Soc. *138*, 778-781. 10.1021/jacs.5b12354.
15. Kar, S., Sen, R., Goeppert, A., and Prakash, G.K.S. (2018). Integrative $CO_2$ Capture and Hydrogenation to Methanol with Reusable Catalyst and Amine: Toward a Carbon Neutral Methanol Economy. J. Am. Chem. Soc. *140*, 1580-1583. 10.1021/jacs.7b12183.
16. Sen, R., Goeppert, A., Kar, S., and Prakash, G.K.S. (2020). Hydroxide Based Integrated $CO_2$ Capture from Air and Conversion to Methanol. J. Am. Chem. Soc. *142*, 4544-4549. 10.1021/jacs.9b12711.
17. Chen, L., Li, F., Zhang, Y., Bentley, C.L., Horne, M., Bond, A.M., and Zhang, J. (2017). Electrochemical Reduction of Carbon Dioxide in a Monoethanolamine Capture Medium. ChemSusChem *10*, 4109-4118. https://doi.org/10.1002/cssc.201701075.

18. Abdinejad, M., Mirza, Z., Zhang, X.-a., and Kraatz, H.-B. (2020). Enhanced Electrocatalytic Activity of Primary Amines for $CO_2$ Reduction Using Copper Electrodes in Aqueous Solution. ACS Sustain. Chem. Eng. *8*, 1715-1720. 10.1021/acssuschemeng.9b06837.
19. Lee, G., Li, Y.C., Kim, J.-Y., Peng, T., Nam, D.-H., Sedighian Rasouli, A., Li, F., Luo, M., Ip, A.H., Joo, Y.-C., and Sargent, E.H. (2021). Electrochemical upgrade of $CO_2$ from amine capture solution. Nat. Energy *6*, 46-53. 10.1038/s41560-020-00735-z.
20. Pérez-Gallent, E., Vankani, C., Sánchez-Martínez, C., Anastasopol, A., and Goetheer, E. (2021). Integrating $CO_2$ Capture with Electrochemical Conversion Using Amine-Based Capture Solvents as Electrolytes. Ind. Eng. Chem. Res. *60*, 4269-4278. 10.1021/acs.iecr.0c05848.
21. Morimoto, T., Nakajima, T., Sawa, S., Nakanishi, R., Imori, D., and Ishitani, O. (2013). $CO_2$ Capture by a Rhenium(I) Complex with the Aid of Triethanolamine. J. Am. Chem. Soc. *135*, 16825-16828. 10.1021/ja409271s.
22. Liao, Y., Cao, S.-W., Yuan, Y., Gu, Q., Zhang, Z., and Xue, C. (2014). Efficient $CO_2$ Capture and Photoreduction by Amine-Functionalized $TiO_2$. Chem. Eur. J. *20*, 10220-10222. https://doi.org/10.1002/chem.201403321.
23. Xia, Y., Tian, Z., Heil, T., Meng, A., Cheng, B., Cao, S., Yu, J., and Antonietti, M. (2019). Highly Selective $CO_2$ Capture and Its Direct Photochemical Conversion on Ordered 2D/1D Heterojunctions. Joule *3*, 2792-2805. https://doi.org/10.1016/j.joule.2019.08.011.
24. Mathias, P.M., Reddy, S., Smith, A., and Afshar, K. (2013). Thermodynamic analysis of $CO_2$ capture solvents. Int. J. Greenh. Gas Control. *19*, 262-270. https://doi.org/10.1016/j.ijggc.2013.09.001.
25. Mahmoudi, H., Mahmoudi, M., Doustdar, O., Jahangiri, H., Tsolakis, A., Gu, S., and LechWyszynski, M. (2017). A review of Fischer Tropsch synthesis process, mechanism, surface chemistry and catalyst formulation. Biofuels Eng. *2*, 11-31. doi:10.1515/bfuel-2017-0002.
26. Huq, F., and Ababneh, D. (2007). Molecular Modelling Analysis of the Metabolic Activation of Ethylene Glycol. J. Pharmacol. Toxicol. *2*, 54-62.
27. García-Abuín, A., Gómez-Díaz, D., López, A.B., Navaza, J.M., and Rumbo, A. (2013). NMR Characterization of Carbon Dioxide Chemical Absorption with Monoethanolamine, Diethanolamine, and Triethanolamine. Ind. Eng. Chem. Res. *52*, 13432-13438. 10.1021/ie4010496.
28. Kar, S., Goeppert, A., Galvan, V., Chowdhury, R., Olah, J., and Prakash, G.K.S. (2018). A Carbon-Neutral $CO_2$ Capture, Conversion, and Utilization Cycle with Low-Temperature Regeneration of Sodium Hydroxide. J. Am. Chem. Soc. *140*, 16873-16876. 10.1021/jacs.8b09325.
29. Chowdhury, F.A., Goto, K., Yamada, H., and Matsuzaki, Y. (2020). A screening study of alcohol solvents for alkanolamine-based $CO_2$ capture. Int. J. Greenh. Gas Control. *99*, 103081. https://doi.org/10.1016/j.ijggc.2020.103081.
30. Sen, R., Koch, C.J., Goeppert, A., and Prakash, G.K.S. (2020). Tertiary Amine-Ethylene Glycol Based Tandem $CO_2$ Capture and Hydrogenation to Methanol: Direct Utilization of Post-Combustion $CO_2$. ChemSusChem *13*, 6318-6322. https://doi.org/10.1002/cssc.202002285.

31. Wu, Y., Jiang, Z., Lu, X., Liang, Y., and Wang, H. (2019). Domino electroreduction of $CO_2$ to methanol on a molecular catalyst. Nature *575*, 639-642. 10.1038/s41586-019-1760-8.
32. Zhang, X., Wu, Z., Zhang, X., Li, L., Li, Y., Xu, H., Li, X., Yu, X., Zhang, Z., Liang, Y., and Wang, H. (2017). Highly selective and active $CO_2$ reduction electrocatalysts based on cobalt phthalocyanine/carbon nanotube hybrid structures. Nat. Commun. *8*, 14675. 10.1038/ncomms14675.
33. Pornrungroj, C., Andrei, V., Rahaman, M., Uswachoke, C., Joyce, H.J., Wright, D.S., and Reisner, E. (2021). Bifunctional Perovskite-$BiVO_4$ Tandem Devices for Uninterrupted Solar and Electrocatalytic Water Splitting Cycles. Adv. Funct. Mater. *31*, 2008182. https://doi.org/10.1002/adfm.202008182.
34. Andrei, V., Ucoski, G.M., Pornrungroj, C., Uswachoke, C., Wang, Q., Achilleos, D.S., Kasap, H., Sokol, K.P., Jagt, R.A., Lu, H., et al. (2022). Floating perovskite-$BiVO_4$ devices for scalable solar fuel production. Nature *608*, 518-522. 10.1038/s41586-022-04978-6.
35. Andrei, V., Hoye, R.L.Z., Crespo-Quesada, M., Bajada, M., Ahmad, S., De Volder, M., Friend, R., and Reisner, E. (2018). Scalable Triple Cation Mixed Halide Perovskite–$BiVO_4$ Tandems for Bias-Free Water Splitting. Adv. Energy Mater. *8*, 1801403. https://doi.org/10.1002/aenm.201801403.
36. Andrei, V., Reuillard, B., and Reisner, E. (2020). Bias-free solar syngas production by integrating a molecular cobalt catalyst with perovskite–$BiVO_4$ tandems. Nat. Mater. *19*, 189-194. 10.1038/s41563-019-0501-6.
37. Rahaman, M., Andrei, V., Pornrungroj, C., Wright, D., Baumberg, J.J., and Reisner, E. (2020). Selective CO production from aqueous $CO_2$ using a $Cu_{96}In_4$ catalyst and its integration into a bias-free solar perovskite–$BiVO_4$ tandem device. Energ. Environ. Sci. *13*, 3536-3543. 10.1039/D0EE01279C.
38. Sharif, H.M.A., Mahmood, N., Wang, S., Hussain, I., Hou, Y.-N., Yang, L.-H., Zhao, X., and Yang, B. (2021). Recent advances in hybrid wet scrubbing techniques for $NO_x$ and $SO_2$ removal: State of the art and future research. Chemosphere *273*, 129695. https://doi.org/10.1016/j.chemosphere.2021.129695.
39. Zhao, M., Xue, P., Liu, J., Liao, J., and Guo, J. (2021). A review of removing SO2 and NOX by wet scrubbing. Sustain. Energy Technol. Assess. *47*, 101451. https://doi.org/10.1016/j.seta.2021.101451.
40. Xu, Y., Edwards, J.P., Zhong, J., O'Brien, C.P., Gabardo, C.M., McCallum, C., Li, J., Dinh, C.-T., Sargent, E.H., and Sinton, D. (2020). Oxygen-tolerant electroproduction of $C_2$ products from simulated flue gas. Energ. Environ. Sci. *13*, 554-561. 10.1039/C9EE03077H.
41. Cheng, Y., Hou, J., and Kang, P. (2021). Integrated Capture and Electroreduction of Flue Gas $CO_2$ to Formate Using Amine Functionalized $SnO_x$ Nanoparticles. ACS Energy Lett. *6*, 3352-3358. 10.1021/acsenergylett.1c01553.
42. Gutiérrez-Sánchez, O., de Mot, B., Daems, N., Bulut, M., Vaes, J., Pant, D., and Breugelmans, T. (2022). Electrochemical Conversion of $CO_2$ from Direct Air Capture Solutions. Energy Fuels, doi: 10.1021/acs.energyfuels.1022c02623. 10.1021/acs.energyfuels.2c02623.

43. Mailhot, B., Morlat-Thérias, S., Ouahioune, M., and Gardette, J.-L. (2005). Study of the Degradation of an Epoxy/Amine Resin, 1. Macromol. Chem. Phys. *206*, 575-584. https://doi.org/10.1002/macp.200400395.
44. Biswas, B., Kandola, B.K., Horrocks, A.R., and Price, D. (2007). A quantitative study of carbon monoxide and carbon dioxide evolution during thermal degradation of flame retarded epoxy resins. Polym. Degrad. Stab. *92*, 765-776. https://doi.org/10.1016/j.polymdegradstab.2007.02.006.
45. Noh, H.-B., Lee, K.-S., Chandra, P., Won, M.-S., and Shim, Y.-B. (2012). Application of a Cu–Co alloy dendrite on glucose and hydrogen peroxide sensors. Electrochim. Acta *61*, 36-43. https://doi.org/10.1016/j.electacta.2011.11.066.